Design Hybrid ARO-SVR Analysis To Predict The Pile Bearing Capacity

Yafan LIU[1*] and Wenjun MA[2,3]

[1] Department of Architectural Engineering, Shijiazhuang College of Applied Technology, Shijiazhuang, Hebei 050000, China
[2] Shijiazhuang Tiedao University, Shijiazhuang, Hebei 050000, China
[3] Hebei Provincial Academy of Emergency Management Scieces, Shijiazhuang, Shijiazhuang Hebei 050000, China
[*] Corresponding author. E-mail: yafandeyouxiang@126.com

Received: Dec. 12, 2023; Accepted: Aug. 12, 2024

The assessment of the load-bearing capacity of piles holds significant importance in the design of pile foundations. This paper presents hybridized support vector regression (SVR) models by utilizing the Artificial Rabbit Optimization (ARO) and the Black Widow Optimization Algorithm (BWOA) to predict the bearing capacity of concrete piles. A repository comprising 472 reports on static load tests conducted on driven piles was employed for the study. The dataset was allocated into three parts: the training set (70%), the validation set (15%), and the testing set (15%). Multiple criteria for assessing quality were utilized to evaluate the effectiveness of the models. The first rank belonged to the SVR model integrated with the ARO algorithm, where it could gain the higher value of R^2 in all of training $(R^2 = 0.9876)$, validating $(R^2 = 0.9778)$, and testing sections $(R^2 = 0.9874)$, and the lowest value of RMSE in all the training (RMSE $= 39.393$), validating (RMSE $= 53.727$) and testing sections (RMSE $= 38.082$). The findings indicate that the suggested model is highly appropriate for predicting the capacity of concrete piles.

Keywords: Concrete piles; Bearing capacity; Estimation; Regression analysis; Artificial Rabbit optimization

http://dx.doi.org/10.6180/jase.202507_28(7).0002

1. Introduction

A pile is a lengthy structural component employed to facilitate the transfer of structural loads to the underlying soils at a depth beneath the base of the structure. Structural loads, such as axial, lateral, and moment loads, exemplify the types of loads encountered. The mechanism of load transmission relies on the resistances offered by the pile toe and pile shaft [1]. In practical applications, the term "deep foundations" is frequently used interchangeably with "pile foundations" [2]. The issue of deep foundation design holds relevance to numerous civil engineering structures, given the increasing prevalence of constructing buildings on soft soils. Pile foundations, which serve to transmit the load of superstructures to the underlying subsoil and bearing layers, are widely employed in this context [3]. However, accurately predicting the settlement of piles proves challenging due to the intricate nature of the consolidation process and pile-soil interaction [4, 5]. Over the past few decades, various approaches encompassing experimental, numerical, and analytical methods have been put forth to estimate pile-bearing capacity [6–13]. Ensuring a high level of accuracy and consistency in these estimations remains of utmost significance [14].

The determination of pile bearing capacity can be achieved through five distinct approaches, including dynamic analysis, high strain dynamic test, pile load test, cone penetration test (CPT), and in situ tests [15–17].

Design guidelines frequently recommend the utilization of the critical depth concept based on static analysis. However, it should be noted that the idealization of the critical depth lacks both theoretical and reliable experimental support, and is in contradiction with physical laws. Dynamic analysis methods, on the other hand, utilize wave mechanics to analyze the hammer-pile-soil system. How-

ever, uncertainties arise from factors such as the impact effect of the hammer, and variations in soil strength during pile driving and loading, which in turn affect the determination of bearing capacity. It is important to highlight that dynamic testing methods require the expertise of an experienced individual, and the estimation of capacity is only possible after the pile has been driven [18]. Although pile load tests are widely regarded as the most accurate and reliable method for ascertaining the bearing capacity of piles, they are often expensive, time-consuming, and may not be justifiable for ordinary or small-scale projects. In recent years, there has been a notable surge in the utilization of in-situ testing techniques in geotechnical design, driven by advancements in in-situ testing instruments and enhanced comprehension of soil behavior [7].

However, as stated by previous research [17], it has been identified that these empirical formulations possess certain limitations and deficiencies [19]. Consequently, there exists a significant requirement for the establishment of precise and reliable models for accurately predicting bearing capacity in order to facilitate the design of pile foundations, particularly when dealing with a limited number of easily determined parameters [20].

Over the course of the past five years, the utilization of machine learning (ML) algorithms has gained significant traction in addressing real-world challenges, specifically within the civil engineering discipline. Through the utilization of ML algorithms, numerous practical issues have been effectively resolved, thereby opening up potential prospects within the infrastructure sector. Furthermore, a variety of ML algorithms have been established, such as the Classification tree, hybrid artificial intelligence methods, ANN (artificial neural network), ANFIS (adaptive neuro-fuzzy inference system), and SVM (support vector machine), to assess technical issues, such as forecasting pile mechanical performance [16].

The attention surrounding the ANN algorithm for addressing design challenges in pile foundation has been noteworthy. As an illustration, Goh et al. [21] displayed an ANN model that predicted the friction capacity of driven piles in clays, utilizing field data collection for training. Similarly, Shahin and Jaksa [22] employed an ANN model to forecast the loading capacity of driven piles and drilled shafts, utilizing a data collection comprising in-situ load tests and CPT results. Additionally, Nawari et al. [23] introduced an ANN algorithm to forecast the settlement analysis of drilled shafts considering Standard Penetration Test (SPT) data and shaft dimensions. An ANN model was developed by Momeni et al. [1] to estimate the axial bearing capacity of concrete piles. The Pile Driving Analyzer (PDA) data obtained from project sites was utilized for this purpose. Furthermore, an ANN algorithm and Random Forest (RF) were devised by Pham et al. [16] to estimate the axial bearing capacity of driven piles. In terms of other ML models, SVR and Particle Swarm Optimization $(PSO-SVR)$, a "nature-inspired" meta-heuristic algorithm, have been utilized to forecast soil shear strength [24]. Moreover, Pham et al. [25] proposed a hybrid ML model that combined RF and PSO $(PSO-RF)$ to forecast the soil's resistance to shear deformation without drainage. These studies have consistently demonstrated the practicality and efficiency of utilizing hybrid ML models were evaluated as effective tools for addressing geotechnical problems, with a specific focus on the prediction of axial bearing capacity in piles.

In view of the recent advancements in ML, it is important to acknowledge certain limitations. ML methods necessitate substantial amounts of structured training data, which must be manually crafted, and real-time learning of these skills is not feasible. Additionally, the generalization capability of ML models remain limited beyond the situations they faced during the training phase. Consequently, ML models can only provide accurate predictions within a specific range of data and may not be applicable in all scenarios [16].

Numerous studies have successfully utilized various ML algorithms to estimate the bearing capacity of foundations. For instance, one study employed an ANFIS and ANN models to estimate the bearing capacity of a thin-walled foundation. This was achieved by utilizing a dataset of 150 samples, resulting in a coefficient of determination (R^2) values of 0.875 and 0.71 , as well as root mean squared error $(RMSE)$ values of 0.048 and 0.529 for ANFIS and ANN, respectively [26]. In another study, Gaussian Process Regression analysis was utilized to calculate the piles' bearing capability. This analysis utilized a dataset of 296 data rows and achieved an R^2 value of 0.84 [27]. Kulkarni and Dewaikar [28] combined the GA algorithm with ANN to model the behavior of rock-socketed piles, utilizing 132 data points. The resulting model yielded an R^2 value of 0.86 and an $RMSE$ value of 0.0093 . In another study, a hybrid model called PSO - ANN used this dataset to analyze the behavior of rock-socketed piles. The model achieved an R^2 value of 0.918 and an RMSE value of 0.063 [29]. Additionally, a comprehensive dataset consisting of 472 samples from experimental efforts was considered in other attempts to develop models [16, 19]. Two different models were used: a hybrid deep neural network (DNN) with a genetic algorithm (GA) and a hybrid whale optimization algorithm (WOA) with extreme gradient boosting (XGB). The $GA-DNN$ model yielded an R^2 value of 0.882

and an $RMSE$ value of 109.965 . On the other hand, the WOA - XGB model performed significantly better, achieving an R^2 value of 0.97 an RMSE value of 64 during the training phase, and an R^2 value of 0.94 and an $RMSE$ value of 87.03 during the testing phase.

In summary, the current research has produced significant contributions, this can be summed up like this:

- In this investigation, 472 pile test results from the entire dataset are used to build as well as verify algorithms aimed at evaluating the bearing capability of piles. It is essential to recognize that previous studies have often focused on restricted datasets. The scholarly study on the assessment of the load-bearing capability of piles has not given sufficient attention to the exploration of hybrid support vector regression (SVR) analysis using advanced algorithms, despite the presence of many proposed models.
- The process of choosing the suitable model, which involves selecting the proper hyperparameters, has significant significance. This study introduces and verifies a novel methodology that integrates the Artificial Rabbit Optimization Algorithm (ARO) and Black Widow Optimization Algorithm ($BWOA$) models with the SVR technique.

Our review of the literature has highlighted several gaps that need to be addressed to gain a deeper insight into the main objective. In order to address these gaps and build upon the existing knowledge, it is crucial to employ a robust methodological framework. The following chapter outlines the research design, data collection methods, and analytical techniques used in this study. This methodology is designed to systematically investigate the underlying factors and provide reliable and valid results.

2. Methodology

2.1. Artificial rabbit optimization (*ARO*)

2.1.1. ARO theory

The ARO procedure is influenced by the survival mechanisms observed in rabbits. Rabbits utilize two primary methods to ensure their survival: detour foraging and random hiding when faced with threats [30]. Detour foraging involves rabbits avoiding feeding on the grass near their nests to protect them from predators. In contrast, they persistently seek out food at a greater distance from their nests. Rabbits possess a wide field of vision, relying on overhead scanning to detect food sources over a large area. This detour foraging strategy can be interpreted as an exploratory behavior. As the Chinese proverb states, "Rabbits do not eat the grass near their own nest." Another adaptive approach for survival employed by rabbits is the act of concealing themselves in an unpredictable manner. Rabbits create multiple burrows in the vicinity of their nests in order to deceive adversaries and facilitate their getaway. When threatened, they haphazardly pick one of the dens as a concealment spot. Rabbits' physical attributes, such as abbreviated front limbs, elongated hind limbs, robust muscles, and resilient tendons, enable them to run swiftly. They can also confuse their enemies by employing zigzag motions, sudden stops, and sharp turns. This second strategy can be seen as exploitation. However, rapid running consumes energy. Therefore, rabbits must dynamically alternate between indirect foraging routes and arbitrary concealment strategies, depending on their energy levels.

2.1.2. ARO numerical model

The incorporates the act of searching for food and concealing oneself approaches of real rabbits, taking into account their energy constraints to transition between these approaches. The numerical representation of the ARO procedure consists of three main components: diversionary foraging (exploration), stochastic concealment (exploitation), and energy constraint. The detailed numerical representation of ARO is addressed in [30].

1. ***Diversionary foraging (exploration)***

   In the ARO algorithm, every rabbit within the collective is assumed to establish their own territory with vegetation and underground shelters. The rabbits engage in random visits to each other's positions to search for food. During foraging, rabbits tend to gather in the vicinity of a food supply to ensure an adequate food intake. The ARO diversionary foraging tactic involves each search individual updating their stance on another randomly chosen subject of the search within the group while also introducing a disturbance. The mathematical model for diversionary foraging in ARO is presented as follows:

$$\begin{aligned}\overrightarrow{v_i}(t+1) =& \overrightarrow{x_j}(t) + R \cdot \left(\overrightarrow{x_i}(t) - \overrightarrow{x_j}(t)\right) \\ &+ \text{round}\left(0.5 \cdot (0.05 + \mathrm{r}_1)\right) \cdot \mathrm{n}_1, \\ &\mathrm{i}, \mathrm{j} = 1, \ldots, \mathrm{n} \text{ and } \mathrm{j} \neq \mathrm{i}\end{aligned} \tag{1}$$

$$R = L \cdot c(24) \tag{2}$$

$$L = \left(e - e^{\left(\frac{t-1}{T}\right)^2}\right) \cdot \sin\left(2\pi r_2\right) \tag{3}$$

$$c(k) = \begin{cases} 1 \text{ if } k == g(l) \\ \text{else} \\ 0 \end{cases} \quad k = 1, \ldots, d \text{ and } l = 1, \ldots, [r_3 \cdot d] \tag{4}$$

$$g = \text{ rand perm } (d) \tag{5}$$

$$n_1 \sim N(0,1)(28) \tag{6}$$

In the context of the *ARO* algorithm, the selected location of the rabbit with the index i at the time $t+1$ is denoted as $\vec{v}_l(t+1)$, while the location of the i^{th} rabbit at time t is represented by $\vec{x}_J(t)$. The variables n and d, respectively, indicate the dimension of the rabbit community and the aspect of the problem. T signifies the maximum quantity of cycles, and $d \bullet e$ represents the ceiling function. The function round is used to round off to the nearest integer. The function rand perm generates a randomized arrangement of numbers ranging covering 1 to d. The variables r_1, r_2, and r_3 are three arbitrary numbers within the variety of $(0,1)$. The variable l denotes the ongoing duration that determines the rate of motion during diversionary foraging. Additionally, n_1 follows a Gaussian dispersion.

Eq. (1) illustrates those searching individuals engage in arbitrary foraging based on the positions of other individuals. This behavior enables a rabbit to venture far from its area and explore the areas of other rabbits. Notably, a rabbit exploring the nests of other rabbits instead of the construction of its nests greatly enhances exploration and ensures the *ARO* algorithm's ability to identify the comprehensive search.

2. *Stochastic concealment (exploitation)*

In the *ARO* algorithm, during each cycle, a rabbit creates d burrows randomly around its current position in every variable in the problem domain. It then selects one of these burrows to hide in, reducing the likelihood of encountering an attack. The j^{th} nest of the i^{th} rabbit is created employing the provided process:

$$\overrightarrow{b_{l,j}}(t) = x_i(t) + H \cdot g \cdot \overrightarrow{x_i}(t), i = 1, \ldots, n \text{ and } j = 1, \ldots, d \tag{7}$$

$$H = \frac{T - t + 1}{T} \cdot r4 \tag{8}$$

$$n_2 \sim N(0,1) \tag{9}$$

$$g(k) = \begin{cases} 1 & \text{if } k = j = \\ 0 & \text{else} \end{cases} \quad k = 1, \ldots, d \tag{10}$$

Based on mathematical Eq. (7), the creation of d burrows occurs in the vicinity of a rabbit across each dimension. The concealment variable, denoted as H, undergoes a linear decrease from 1 to $1/T$, accompanied by unpredictable perturbations throughout the cycles. This variable governs the initial production of burrows within a broader vicinity of the rabbit. As the process advances, the size of this neighborhood gradually diminishes. Rabbits employ a random selection process to choose a burrow from their available options for a location for protection. To analytically represent this stochastic concealment approach, the subsequent equations are employed:

$$\overrightarrow{\mathrm{v}_l}(\mathrm{t}+1) = \mathrm{x}_i(\mathrm{t}) + \mathrm{R} \cdot \left(\mathrm{r}_4 \cdot \overrightarrow{\mathrm{b}_{1,r}}(\mathrm{t}) - \overrightarrow{\mathrm{x}_l}(\mathrm{t})\right), \mathrm{i} = 1, \ldots, \mathrm{n} \tag{11}$$

$$\mathrm{g}_r(\mathrm{k}) = \begin{cases} 1 \text{ if } \mathrm{k} == [\mathrm{r}_5 & \cdot \mathrm{d}] \\ 0 & \text{else} \end{cases} \quad \mathrm{k} = 1, \ldots, \mathrm{d} \tag{12}$$

$$\overrightarrow{\mathrm{b}_{1,r}}(\mathrm{t}) = \overrightarrow{\mathrm{x}_l}(\mathrm{t}) + \mathrm{H} \cdot \mathrm{g}_r \cdot \overrightarrow{\mathrm{x}_l}(\mathrm{t}) \tag{13}$$

In the given context, variable $\overrightarrow{\mathrm{b}_{1,\mathrm{r}}}(\mathrm{t})$ denotes a burrow that is arbitrarily chosen by the i^{th} search individuals for the purpose of taking cover in its d burrows. The variables r_4 and r_5 represent two random numbers within the range of $(0,1)$. Referring to Eq. (11), the i^{th} the candidate will attempt to adjust its location in relation to the arbitrarily chosen underground dwelling from its set of d dens. Once either the diversionary foraging or concealment is successfully accomplished, the position modification of the i^{th} rabbit can be described as:

$$\overrightarrow{x_l}(t+1) = \begin{cases} \overrightarrow{x_l}(t) f\left(\overrightarrow{x_l}(t)\right) \leq f\left(\overrightarrow{v_l}(t+1)\right) \\ \overrightarrow{v_l}(t+1) f\left(\overrightarrow{x_l}(t)\right) > f\left(\overrightarrow{v_l}(t+1)\right) \end{cases} \tag{14}$$

The aforementioned equation indicates that if the suitability of the potential location for the i^{th} rabbit surpasses that of the ongoing position. The rabbit will leave its existing location and settle at the potential location produced by either Eq. (1) or Eq. (11).

Additionally, the shift from exploring to exploiting is facilitated through the calculation of an energy parameter in the *ARO* algorithm. This energy factor is determined according to the provided equation, with r representing a random number within the range of $(0,1)$:

$$A(t) = 4\left(1 - \frac{t}{T}\right) \ln \frac{1}{r} \tag{15}$$

In the ARO algorithm, the behavior of rabbits is influenced by the energy factor $A(t)$. When $A(t)$ exceeds 1 , rabbits engage in random exploration to discover foraging areas during the exploration phase. Conversely, when $A(t)$ is less than or equal to 1 , rabbits are motivated to exploit their burrows randomly during the exploitation phase, resulting in random hiding behavior. The transition between diversionary foraging and concealment is determined by the value of A. As iterations progress, the energy factor A decreases, enabling individuals within the community to switch in the context of diversionary foraging and random concealment tactics. The current revisions continue prior to the stopping condition being met, at which point the optimal answer is obtained. The algorithmic representation for the ARO algorithm is presented in Algorithm 1.

2.2. Black widow optimization algorithm ($BWOA$)

$BWOA$ [31], is an innovative metaheuristic approach designed to tackle complex numerical optimization problems. Drawing inspiration from the distinctive mating behavior exhibited by black widow spiders, this algorithm demonstrates superior performance when compared to alternative evolutionary algorithms. The remarkable characteristics of the black widow spider's mating behavior contribute to the $BWOA$ algorithm's ability to converge rapidly while effectively circumventing local optima. Consequently, the $BWOA$ algorithm presents a practical and viable solution for addressing diverse optimization problems characterized by numerous local optima.

Due to its relatively recent introduction, the utilization of this algorithm in the oil industry has been limited. However, it has demonstrated successful implementation in optimization endeavors within other domains, including image segmentation [32] and biotechnology research [33].

In order to determine the optimal solution, the $BWOA$ algorithm follows a series of distinct steps. Firstly, a randomly generated starting number of black widow spiders in a given area is established, and the fitness of each individual is assessed and evaluated accordingly. It is important to note that within the framework of this algorithm, every individual black widow spider represents a potential solution to the given problem, with the position of wells being explicitly indicated in each spider. Subsequently, spiders are randomly selected as parents for the purpose of procreation. As a result, a novel iteration emerges, marking the inception of a new era of black widow spiders, which serve as potential solutions, through the utilization of $BWOA$ operators such as crossover, mutation, and cannibalism. The population is then updated based on the newly generated spiders. This entire process is repeated until the specified stopping conditions are met.

The initial phase of the BWO algorithm involves the stochastic generation of an initial population of spiders. In the context of the BWO algorithm, each spider symbolizes a prospective solution to the given problem. Subsequently, the procreation phase is initiated, wherein parent spiders are randomly selected for formatting. The production of progeny is governed by the subsequent formula:

$$y_1 = \alpha \times x_1 + (1 - \alpha) \times x_2 \tag{16}$$

Where y_1 and y_2 represent the offspring, x_1 and x_2 denote the parental individuals, and α symbolizes a randomly generated array. This process is iterated $\frac{N_{var}}{2}$ times for each pair of parents. The determination of parent selection is accomplished through the utilization of the Procreating Rate (PR) technique, which governs the number of parents chosen. Following the creation of a recent wave of spiders, the subsequent step involves cannibalism, wherein the fittest spiders are retained within the population based on the Cannibalism Rate (CR). Prior to updating the population, a mutation phase is executed to ascertain the count of genetic variations. This iterative methodology continues until the merging requirement is satisfied. Fig. 1 presents the flowchart of the $BWOA$.

It is important to acknowledge the presence of three distinct forms of self-predation within this computational procedure. The initial form, known as reproductive self-predation, transpires when a female black widow spider consumes a male black widow spider either in the course of or following the reproductive interaction. The fitness values of the male and female spiders serve as a basis for their characterization, with the female typically possessing a higher fitness value. Following the reproductive phase, the spider displaying inferior fitness (the male spider) is eradicated within the population. Additionally, the fitness level is utilized to ascertain the potency or vulnerability of juvenile spiders. Fratricidal behavior, an alternative form of cannibalistic behavior, involves enhanced baby spiders (those with superior fitness levels) consuming their weaker siblings. It is worth acknowledging the presence of a larger quantity of less powerful siblings that are removed is adjusted by the CR. In certain instances, a third form of autophagy is noticed, wherein the offspring spiders feed on their maternal figures.

It is important to acknowledge the presence of three distinct forms of self-predation within this computational procedure. The initial form, known as reproductive self-predation, transpires when a female black widow spider consumes a male black widow spider either in the course of or following the reproductive interaction. The fitness

Algorithm 1. Comparison of time performance and performance with different superpixel methods

$-Randomly\ assign\ a\ group\ of\ rabbits\ X_i(solutions)\ and\ assess\ their\ fitness\ (Fit),\ with$
X_{best} being the currently discovered optimal solution.
$-$***While*** *the stopping condition is not met,*
$-$***for*** *each individual* X_i*, execute the following steps :*
$-Compute\ the\ energy\ factor\ A\ by\ utilizing\ the\ Eq.\ (15)$
If $A > 1$
$-Select\ an\ individual\ rabbit\ randomly\ from\ the\ others.$
$-Determine\ R\ using\ Eqs.\ (2)to\ (6).$
$-Execute\ detour\ foraging\ using\ Eq.\ (1).$
$-Compute\ the\ fitness\ Fit_i.$
$-Adjust\ the\ current\ individual's\ position\ using\ Eq.\ (14).$
Else
$-Create\ d\ burrows\ and\ randomly\ select\ one\ for\ hiding\ by\ using\ Eq.\ (13).$
$-Implement\ random\ hiding\ using\ Eq.\ (11).$
$-Compute\ the\ fitness\ Fit_i.$
$-Update\ the\ individual's\ position\ using\ Eq.\ (14).$
End If
$-Update\ the\ best\ solution\ found\ thus\ far,\ X_{best}.$
End For
End While
-Return X_{best}

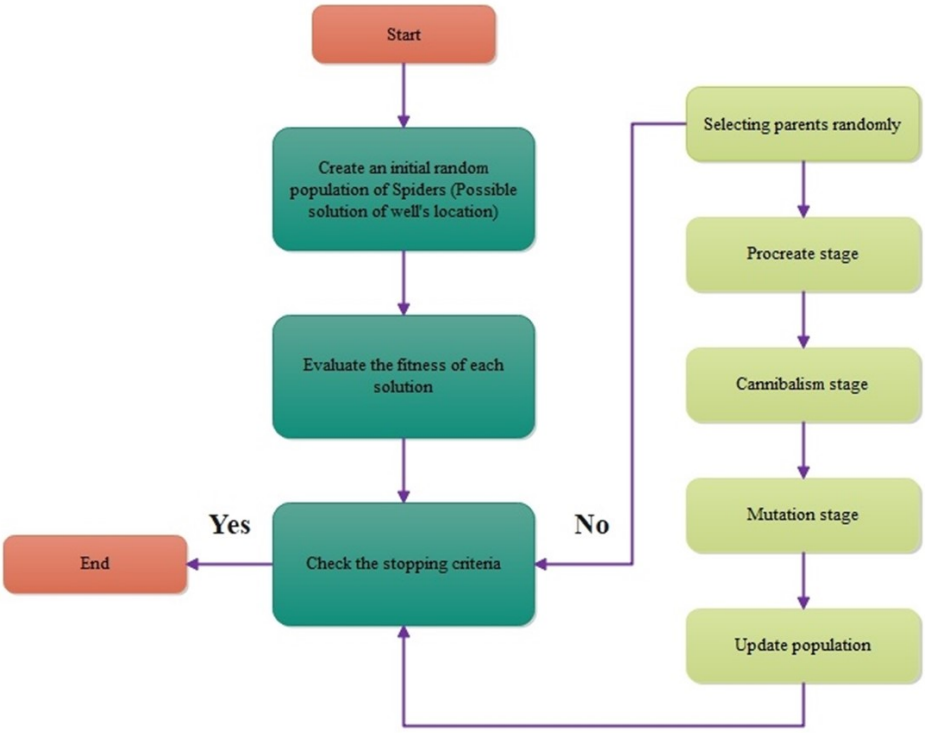

Fig. 1. The flowchart of the black widow optimization algorithm.

values of the male and female spiders serve as a basis for their characterization, with the female typically possessing a higher fitness value. Following the reproductive phase, the spider displaying inferior fitness (the male spider) is eradicated within the population. Additionally, the fitness level is utilized to ascertain the potency or vulnerability of juvenile spiders. Fratricidal behavior, an alternative form of cannibalistic behavior, involves enhanced baby spiders (those with superior fitness levels) consuming their weaker siblings. It is worth acknowledging the presence of a larger quantity of less powerful siblings that are removed is adjusted by the CR. In certain instances, a third form of

autophagy is noticed, wherein the offspring spiders feed on their maternal figures.

2.3. Support vector regression (*SVR*)

The Support Vector Machine (SVM) is a widely used and promising estimator that was initially proposed in 1995 [34]. The core concept and theoretical framework of SVM are based on the selection of support vectors, which are essential in determining how the model is configured as well as the corresponding parameters. In the context of regression, the construction of an SVM estimator (f) involves a specific procedure, which can be expressed as follows:

$$f(x) = w\varphi(x) + b \tag{17}$$

In the context of the SVM, the weight vector is denoted as " w " and the bias term as " b ". Additionally, the function φ represents a mapping from the domain of given data to a higherdimensional feature region. Vapnik introduced a mathematical expression improving lenticular efficiency, incorporating the ε mathematical operation. The numerical expression for this objective function is elucidated as follows:

$$\begin{array}{l} \mathrm{Min}_{\mathrm{w,b},\xi,\xi^*} \quad \frac{1}{2}\|\mathrm{w}\|^2 + \mathrm{C}\sum_{\mathrm{k}=1}^{\mathrm{N}}\left(\xi_\mathrm{k} + \xi_\mathrm{k}^*\right) \\ \text{Subjected to} \quad \begin{cases} \mathrm{y_k} - \mathrm{W^T}\varphi\left(\mathrm{X_k}\right) - \mathrm{b} \le \varepsilon + \xi_\mathrm{k} \\ \mathrm{W^T}\varphi\left(\mathrm{X_k}\right) + \mathrm{b} - \mathrm{y_k} \le \varepsilon + \xi_\mathrm{k}^* \\ \xi_\mathrm{k}, \xi_\mathrm{k}^* \ge 0 \end{cases} \quad \mathrm{k} = \\ 1, 2, \ldots.., N \end{array} \tag{18}$$

In the context of this study, the variables ξk and ξk^* represent the calculation errors determined utilizing the ε mathematical operation. The parameter C is a beneficial compromise element that influences the severity of experimental errors. The optimization criterion can be reformulated by employing the Lagrangian multipliers $(\alpha, \alpha*)$ as described in the following manner:

$$\begin{array}{l} \max\limits_{\alpha,\alpha^*} \begin{cases} -1/2\sum_{k,l=1}^{N}\left(\alpha_k - \alpha_k^*\right)\left(\alpha_l - \alpha_l^*\right)K\left(X_k, X_l\right) \\ -\varepsilon\sum_{k=1}^{N}\left(\alpha_k + \alpha_k^*\right) + \sum_{k=1}^{N} y_k\left(\alpha_k - \alpha_l^*\right) \end{cases} \\ \text{Subject t0} \\ \begin{cases} \sum_{k=1}^{N}\left(\alpha_k - \alpha_k^*\right) = 0 \\ 0 \le \alpha_k, \alpha_k^* \le C \end{cases} \\ \text{to obtain} \\ \sum\limits_{k=1}^{N}\left(\alpha_k - \alpha_k^*\right)K\left(X, X_k\right) + b \end{array} \tag{19}$$

In the context of this research, the kernel function is denoted as " K " and the number of support vectors as " n ". For this study, the algorithm employed a kernel function that utilized a radial basis with a scaling factor σ. The radial basis kernel function can be defined as follows:

$$K\left(X_k, X_t\right) = \exp\left(-\frac{\|X_k - X_t\|^2}{2\sigma^2}\right) \tag{20}$$

The parameters of the (SVR) model, namely C, ε, and σ, were optimized using the ARO, and BWOA algorithms. The implementation of the SVR modeling was carried out using MATLAB software.

2.4. Performance evaluation indices

The following statistical metrics have been calculated to assess the models' performance. A higher level of accuracy is demonstrated by lower values of $RMSE, RAE, RRSE$, and PI. Furthermore, a higher value of R^2 indicates superior performance.

- Coefficient of determination $\left(R^2\right)$

$$R^2 = \left(\frac{\sum_{d=1}^{\mathrm{D}}\left(\mathrm{m_d} - \overline{\mathrm{m}}\right)\left(\mathrm{z_d} - \overline{\mathrm{z}}\right)}{\sqrt{\left[\sum_{\mathrm{d}=1}^{\mathrm{D}}\left(\mathrm{m_P} - \mathrm{m}\right)^2\right]\left[\sum_{\mathrm{d}=1}^{\mathrm{D}}\left(\mathrm{z_d} - \overline{\mathrm{z}}\right)^2\right]}}\right)^2 \tag{21}$$

- Root-mean-square error (RMSE)

$$\mathrm{RMSE} = \sqrt{\frac{1}{\mathrm{D}}\sum_{\mathrm{d}=1}^{\mathrm{D}}\left(\mathrm{z_d} - \mathrm{m_d}\right)^2} \tag{22}$$

- Relative absolute error (RAE)

$$\mathrm{RAE} = \frac{\sum_{\mathrm{d}=1}^{\mathrm{D}}\left|\mathrm{m_d} - \mathrm{z_d}\right|}{\sum_{\mathrm{d}=1}^{\mathrm{D}}\left|\mathrm{m_d} - \overline{\mathrm{m}}\right|} \tag{23}$$

- Root relative squared error (RRSE)

$$\mathrm{RRSE} = \sqrt{\frac{\sum_{\mathrm{d}=1}^{\mathrm{D}}\left(\mathrm{m_d} - \mathrm{z_d}\right)^2}{\sum_{\mathrm{d}=1}^{\mathrm{D}}\left(\mathrm{m_d} - \overline{\mathrm{m}}\right)^2}} \tag{24}$$

- Performance index (PI)

$$\mathrm{PI} = \frac{1}{\overline{\mathrm{m}}}\frac{\mathrm{RMSE}}{\sqrt{\mathrm{R}^2 + 1}} \tag{25}$$

The observations, the average of the observations, the simulations, and the average of the simulations are represented by the variables $\mathrm{m_d}, \overline{\mathrm{m}}, \mathrm{z_d}$, and $\overline{\mathrm{z}}$ in these equations, in that order. D also displays the overall count of datasets.

3. Results and discussion

To train and assess the hybrid SVR analysis outlined in this scholarly article, a dataset comprising static load test results of driven reinforced concrete piles is utilized. This dataset, obtained from previous studies [16], consists of 472 entries and is of substantial size, making it suitable for the development and validation of complex machine-learning models. The experimental setup involved the use of hydraulic pile-driving machines to drive precast piles with closed tips into soil layers, thereby measuring the capacity of the piles. The input variables considered in this study include: 1) the measurement of the pile (In_1 in millimeters), 2) the depth of the initial soil layer in which the piles are embedded (In_2 in meters), 3) the depth of the second soil layer in which the piles are embedded (In_3 in meters), 4) the thickness of the third soil layer in which the piles are embedded (In_4 in meters), 5) the pile top elevation (In_5 in meters), 6) the natural ground elevation (I_6 in meters), 7) the elevation of an additional part of the pile top (In_7 in meters), 8) the depth of the pile tip (In_8 in meters), 9) the mean SPT blow count recorded throughout the whole pile shaft (I_9), as well as10) the average SPT blow count at the pile tip (I_{10}). Table 1 provides a summary of these ten input factors (referred to as In_1 to In_{10}) used for predicting the dependent variable, which represents the axial pilebearing capacity.

The dataset, consisting of 472 rows, was divided into three separate groups: the testing set (also comprising 15% of the records or 71 rows), the validation set (consisting of 15% of the records, or 71 rows), as well as the training set (comprising 70% of the records, or 330 rows). The selection of data points from the larger database was performed randomly, following a normal distribution. Statistical analysis was conducted to assess the suitability of the input parameters. Furthermore, Fig. 2 depicts distribution charts illustrating the characteristics of the input and output variables.

The Pearson correlation coefficient serves as a statistical tool to evaluate the magnitude and orientation of the association between two variables. It gauges how much of a consistent linear pattern the data points in a scatterplot show [35]. The coefficient has a range of -1 to +1 , in which positive values signify a direct association between variables, suggesting that the two variables tend to increase together as one increases. Negative values, on the other hand, signify an inverse relationship in which a rise in one variable is accompanied by a fall in another. Values closer to +1 or -1 suggest a strong linear relationship, while values closer to 0 suggest a weak or negligible linear relationship. In this study, the correlation values between the variables are generally high, with few exceptions (Fig. 3). For instance, there is a strong positive correlation of 0.99 between In_3 and In_8. Conversely, the largest negative correlation, -0.96 , is noted between In_2 as well as In_5. However, it is worth noting that the study may have limitations in effectively capturing the effects of major positive or negative Pearson correlation coefficient variables, suggesting a potential need for a more robust methodology. Nonetheless, incorporating these variables into models can potentially enhance accuracy.

3.1. Results

As stated in this study, hybridized SVR models were used to evaluate the bearing capacity of concrete piles. The hybrid models are referred to as SVR_{ARO} and SVR_{BWOA}, were employed to calculate criteria as performance indices by utilizing ARO and BWOA techniques. The assessment and computation of the bearing capacity of concrete piles were performed during the stages of training, validating, and testing the created mechanisms SVR_{ARO} and SVR_{BWOA} techniques, as depicted in Fig. 4. In Fig. 4, the error distribution is displayed on the right side. To evaluate the effectiveness of SVR_{ARO} as well as SVR_{BWOA} in predicting the procedure, various metrics including $R^2, RMSE, RAE$, RRSE , and PI were utilized, as shown in Table 2. Additionally, the $XGB, WOA-XGB$, and $GA-DLNN$ developed models were evaluated for reliability, and effectiveness according to the findings of this investigation, with a primary focus on their performance. These research outcomes were compared to those of previous research studies [16] and [19].

According to the collected data, it appears that both the SVR_{ARO} and SVR_{BWOA} models exhibit considerable potential in accurately predicting the bearing capacity of piles. During the training phase, the SVR_{ARO} model achieved R^2 values of 0.9876 , while during the validation phase, the values were 0.9778 , and during the testing phase, they were 0.9874 . Similarly, the SVR_{BWOA} model attained R^2 values of 0.9751 during training, 0.9663 during validation, and 0.972 during testing. However, relying solely on a single metric for evaluating the reliability of a model is insufficient. To ensure a comprehensive assessment, it is crucial to conduct a thorough analysis of various measures, including but not limited to $RSME$, RAE, $RRSE$, and PI. When comparing the reported percentages for SVR_{ARO} and SVR_{BWOA} across multiple metrics, it becomes evident that SVR_{ARO} exhibits a significant decrease in performance compared to SVR_{BWOA}. This decline in performance highlights the remarkable accuracy demonstrated by SVR_{ARO} in determining the concrete piles' bearing capability.

Table 1. Descriptive statistics of variables applied to models.

Phase	Metric							
	Minimum	Maximum	Standard deviation	Range	Skewness	Kurtosis	Average	Median
Inputs								
Diameter of the pile (mm) (In_1)								
Training	300	400	48.432	100	-0.515	-1.745	362.424	400
Validating	300	400	48.546	100	-0.504	-1.798	361.972	400
Testing	300	400	44.9823	100	-0.9917	-1.0468	371.831	400
The first soil layer that the pile embedded's thickness (m) (In_2)								
Training	3.4	5.72	0.491	2.32	0.642	-0.730	3.821	3.45
Validating	3.4	4.45	0.447	1.05	0.372	-1.815	3.794	3.45
Testing	3.4	4.75	0.46495	1.35	0.1379	-1.756	3.87746	3.85
The thickness of the second Soil layer that pile embedded (m) (In_3)								
Training	1.5	8	1.574	6.5	-0.946	0.517	6.594	7.305
Validating	1.71	8	1.700	6.29	-1.029	0.638	6.532	7.3
Testing	1.66	8	1.83948	6.34	-1.2861	0.92027	6.5569	7.36
The thickness of the third Soil layer that pile embedded (m) (In_4)								
Training	0	1.69	0.450	1.69	0.893	-0.984	0.321	0
Validating	0	1.13	0.446	1.13	0.856	-1.167	0.326	0
Testing	0	1.22	0.48996	1.22	0.63525	-1.5594	0.38338	0
Elevation of the pile top (m) (In_5)								
Training	0.68	3.4	0.619	2.72	-0.393	-1.388	2.812	2.95
Validating	1.95	3.4	0.609	1.45	-0.362	-1.700	2.825	2.95
Testing	1.95	3.4	0.60256	1.45	-0.0936	-1.802	2.74225	2.95
Elevation of natural ground (m) (I_6)								
Training	3.04	4.12	0.080	1.08	1.310	13.141	3.495	3.48
Validating	3.26	3.67	0.078	0.41	-0.203	1.031	3.490	3.48
Testing	3.21	3.72	0.07878	0.51	-0.6016	3.06421	3.50169	3.5
The extra segment pile top elevation (m) (In_7)								
Training	1.03	4.05	0.598	3.02	-0.667	-0.982	2.929	3.355
Validating	2	3.58	0.577	1.58	-0.532	-1.458	2.914	3.04
Testing	1.99	4.35	0.61997	2.36	-0.2142	-1.3344	2.87549	2.98
The depth of the pile tip (m) (In_8)								
Training	8.3	16.09	1.733	7.79	-0.693	-0.014	13.547	14.105
Validating	8.51	15.53	1.848	7.02	-0.798	0.143	13.478	14.1
Testing	8.46	15.62	2.02017	7.16	-1.0291	0.34365	13.56	14.16
Along the pile shaft, the average SPT blow count (In_9)								
Training	5.6	15.41	2.220	9.81	-0.156	-1.234	10.746	10.8
Validating	5.81	13.49	2.291	7.68	-0.203	-1.192	10.653	10.72
Testing	5.76	13.57	2.41719	7.81	-0.4566	-0.9812	10.8177	11.21
The mean SPT blow count at the summit of the pile (In_{10})								
Training	4.38	7.73	0.617	3.35	-1.926	5.366	7.064	7.115
Validating	4.56	7.7	0.685	3.14	-2.111	5.405	7.047	7.2
Testing	4.52	7.75	0.80459	3.23	-1.9101	3.43106	7.02746	7.27
Output								
The pile's axial bearing capacity load (kN)								
Training	423.9	1551	354.039	1127.1	-0.090	-1.686	987.007	1068.8
Validating	407.2	1551	360.570	1143.8	-0.028	-1.625	956.177	1056
Testing	423.9	1551	337.617	1127.1	-0.1526	-1.5152	999.186	1119.7

To evaluate the reliability of the models, a thorough assessment was conducted by comparing them with existing literature, specifically considering the XGB [19], WOAXGB [19], and $GA-DLNN$ [16] models. Table 2 provides a comprehensive analysis, revealing that the SVR_{ARO}, introduced in this investigation, showed positive results when compared to earlier studies covered in the body of current literature. The evaluation employed consistent metrics, namely R^2 and $RMSE$, for the training, validation, and testing datasets. The SVR_{ARO} model demonstrated higher R^2 values and lower $RMSE$ compared to the XGB [19], $WOA-XGB$ [19], and $GA-DLNN$ [16] models, indicating enhanced precision and robustness in its findings. For instance, the $WOA-XGB$ model exhibited an increase in

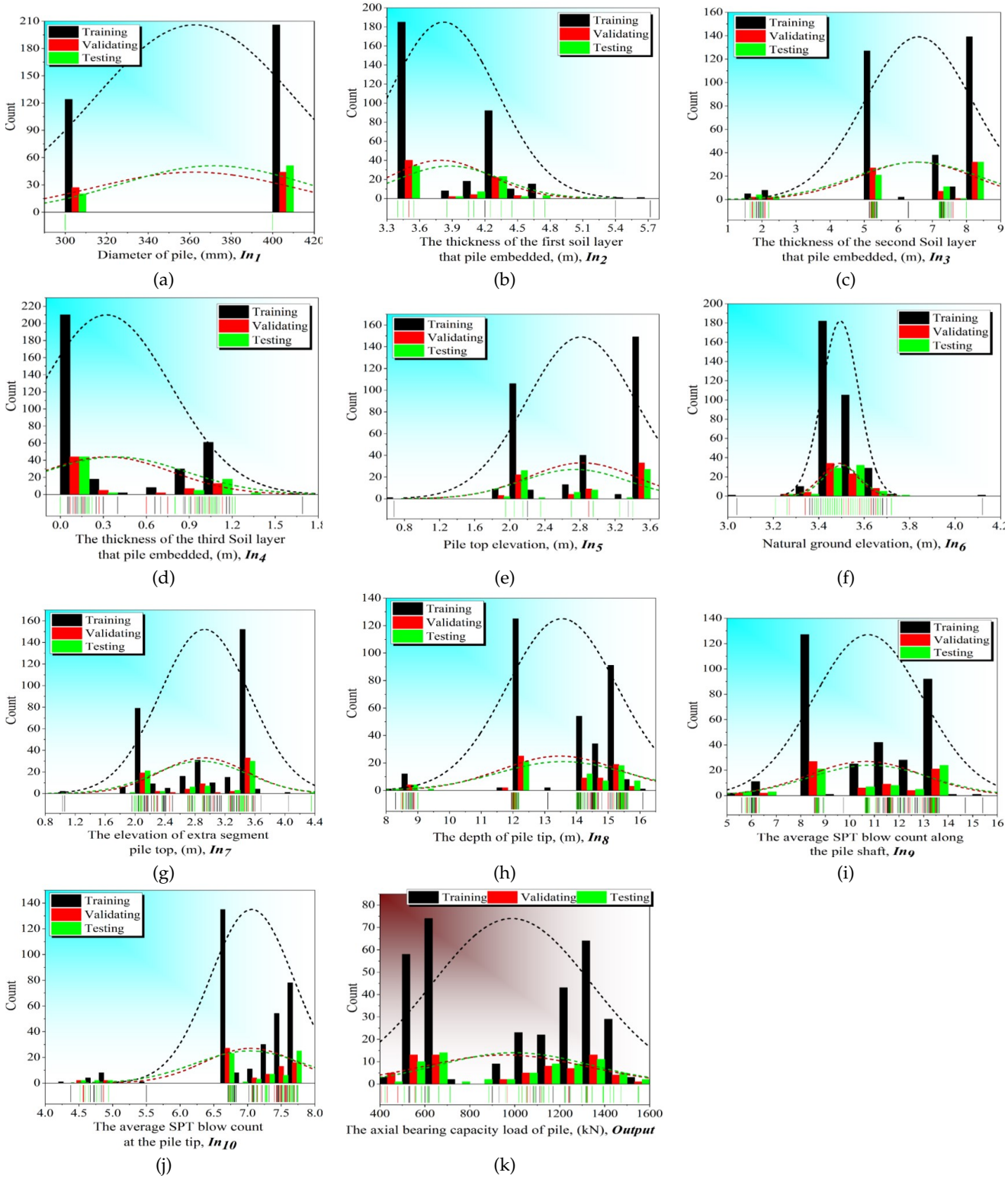

Fig. 2. Distribution of variables introduced to models in the Training, validating, and Testing phases.

R^2 from 0.94 to 0.9874 during the testing stage and from 0.97 to 0.9876 during the training stage.

Furthermore, the training stage's $RMSE$ error measurements showed a decline from 62.74 to 39.395, and the testing stage's from 87.72 to 38.082 . A detailed evaluation of the SVR_{ARO} model and the $GA-DLNN$ [16] model can

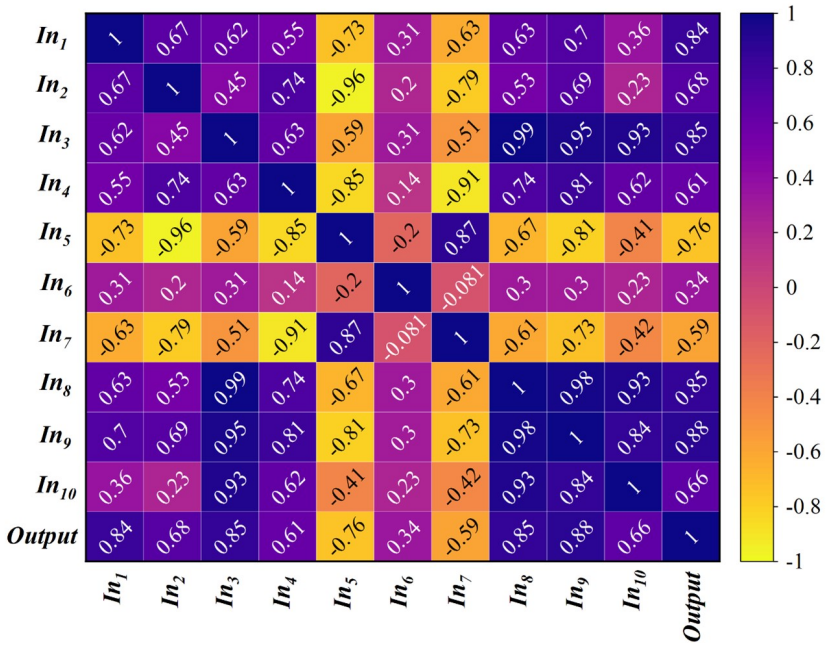

Fig. 3. Correlation coefficient values.

Table 2. The performance of models.

Data phase	Metrics										Total score
	R^2	Score	RMSE	Score	RAE	Score	RRSE	Score	PI	Score	
Training											
SVR_{ARO}	0.9876	2	39.395	2	0.0615	2		2		2	10
SVR_{BWOA}	0.9751	1	55.847	1	0.1121	1	0.158	1	0.028	1	5
XGB [19]	0.99		39.64								
WOA - XGB [19]	0.97		62.74								
GA -DLNN [16]	0.944		83.593								
Validating											
SVR_{ARO}	0.9778	2	53.727	2	0.074	2	0.149	2	0.028	2	10
SVR_{BWOA}	0.9663	1	66.33	1	0.125	1	0.184	1	0.035	1	5
$GA-DLNN$ [16]	0.923		95.118								
Testing											
SVR_{ARO}	0.9874	2	38.082	2	0.0659	2	0.1128	2	0.019	2	10
SVR_{BWOA}	0.972	1	56.48	1	0.122	1	0.1673	1	0.028	1	5
XGB [19]	0.92		101.3								
$WOA-XGB$ [19]	0.94		87.72								
$GA-DLNN$ [16]	0.887		110.17								

be undertaken, considering the improvements observed in the training, validation, and testing datasets, including an increase in R^2 values and a decrease in RMSE values.

4. Conclusion

The objective of this paper was to scrutinize the practicality of hybridized support vector regression (SVR) models with the aim of estimating the bearing capacity of concrete piles. To this aim, a dataset including 472 samples collected from published papers carried out experimental tests. For this target and employing suggested models, different hybridized regression analyses were produced, where the optimal values of main and determinant attributes of SVR were explored by several metaheuristic optimization algorithms such as Artificial Rabbit Optimization (ARO) and Black Widow Optimization Algorithm ($BWOA$), called SVR_{ARO} and SVR_{BWOA}. In order to provide a reliable conclusion, various statistical criteria should be calculated and analyzed, as well as evaluating the improvement of accuracy with the literature. The primary findings are as follows:

The calculated indices as performance indices present

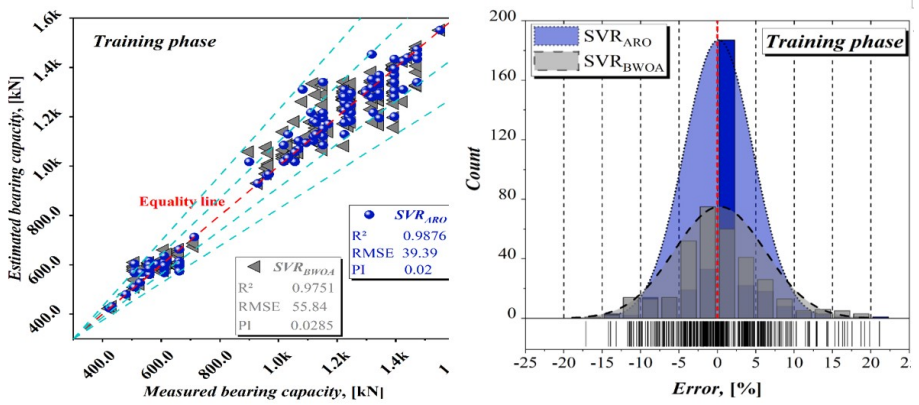

(a)

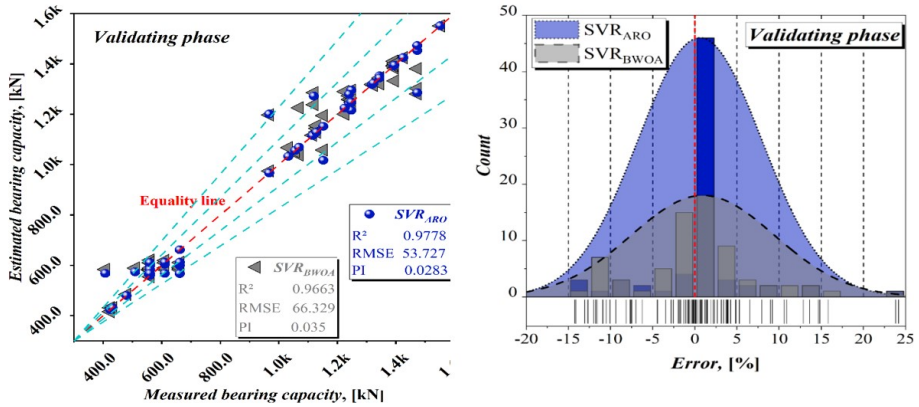

(b)

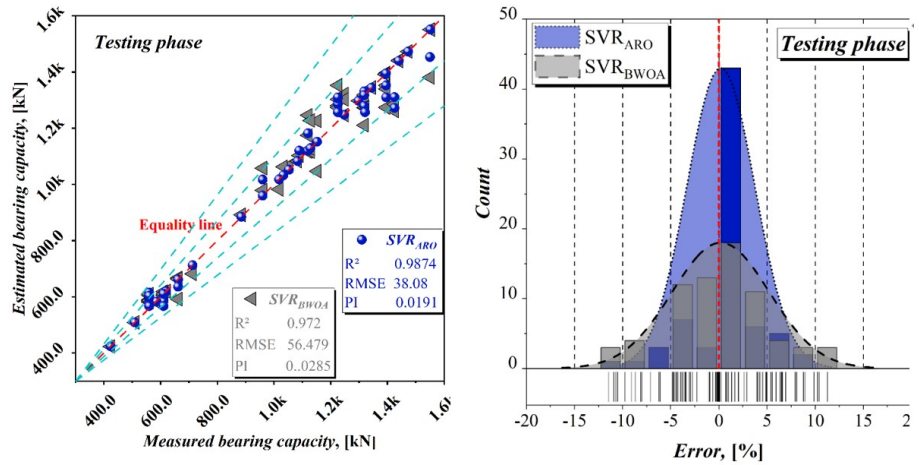

(c)

Fig. 4. Findings of the coupled SVR: (a) Training, (b) Validating, and (c) Testing.

that both hybridized SVR models have reasonable capability in the determination of the bearing capacity of concrete piles. Based on all criteria, SVR_{BWOA} stands in the second rank after SVR_{ARO}, with gaining the R^2 and $RMSE$ at 0.9751 and 55.847 for training, 0.9663 and 66.33 for validating, and 0.972 and 56.48 for testing sections, respectively. The first rank belonged to the SVR model integrated with the ARO algorithm, where it could gain the higher value of R^2 in all of training $(R^2 = 0.9876)$, validating $(R^2 = 0.9778)$, and testing sections $(R^2 = 0.9874)$, and the lowest value of $RMSE$ in all the training $(RMSE = 39.393)$, validating $(RMSE = 53.727)$ and testing sections

($RMSE = 38.082$).

It is evident from the performance of model results that SVR_{ARO} model demonstrated higher R^2 values and lower RMSE compared to the XGB [19], $WOA - XGB$ [19], and $GA - DLNN$ [16] models, indicating enhanced precision and robustness in its findings. For instance, the $WOA - XGB$ model exhibited an increase in R^2 from 0.94 to 0.9874 during the testing stage and from 0.97 to 0.9876 during the training stage. Therefore, the hybridized SVR_{ARO} the model could receive the proper accuracy in comparison with other models as well as literature.

References

[1] E. Momeni, R. Nazir, D. J. Armaghani, and H. Maizir, (2015) *"Application of artificial neural network for predicting shaft and tip resistances of concrete piles"* **Earth Sciences Research Journal *19***: 85–93. DOI: 10.15446/esrj.v19n1.38712.

[2] M. Drusa, F. Gago, and J. Vlček, (2016) *"Contribution to estimating bearing capacity of pile in clayey soils"* **Civil and Environmental Engineering *12***: 128–136. DOI: 10.1515/cee-2016-0018.

[3] F. P. Nejad and M. B. Jaksa, (2017) *"Load-settlement behavior modeling of single piles using artificial neural networks and CPT data"* **Computers and Geotechnics *89***: 9–21. DOI: 10.1016/j.compgeo.2017.04.003.

[4] Z. Buzrukov, I. Yakubjanov, and M. Umataliev. "Features of the joint work of structures and pile foundations on loess foundations". In: ***264***. EDP Sciences, 2021, 02048. DOI: 10.1051/e3sconf/202126402048.

[5] K. Józefiak, A. Zbiciak, M. Maślakowski, and T. Piotrowski, (2015) *"Numerical modelling and bearing capacity analysis of pile foundation"* **Procedia Engineering *111***: 356–363. DOI: 10.1016/j.proeng.2015.07.101.

[6] G. G. Meyerhof, (1976) *"Bearing capacity and settlement of pile foundations"* **Journal of the Geotechnical Engineering Division *102***: 197–228. DOI: 10.1061/AJGEB6.0000243.

[7] I. Shooshpasha, A. Hasanzadeh, and A. Taghavi, (2013) *"Prediction of the axial bearing capacity of piles by SPT-based and numerical design methods"* **Geomate Journal *4***: 560–564. DOI: 10.21660/2013.8.2118.

[8] X. J. Chai, K. Deng, C. F. He, and Y. F. Xiong, (2021) *"Laboratory Model Tests on Consolidation Performance of Soil Column with Drained-Timber Rod"* **Advances in Civil Engineering *2021***: 6698894. DOI: 10.1155/2021/6698894.

[9] G. S. Budi, M. Kosasi, and D. H. Wijaya, (2015) *"Bearing capacity of pile foundations embedded in clays and sands layer predicted using PDA test and static load test"* **Procedia Engineering *125***: 406–410. DOI: 10.1016/j.proeng.2015.11.101.

[10] W. Kozłowski and D. Niemczynski, (2016) *"Methods for estimating the load bearing capacity of pile foundation using the results of penetration tests-case study of road viaduct foundation"* **Procedia engineering *161***: 1001–1006. DOI: 10.1016/j.proeng.2016.08.839.

[11] M. Amjad, I. Ahmad, M. Ahmad, P. Wróblewski, P. Kamiński, and U. Amjad, (2022) *"Prediction of pile bearing capacity using XGBoost algorithm: modeling and performance evaluation"* **Applied Sciences *12***: 2126. DOI: 10.3390/app12042126.

[12] B. Ma, Z. Li, K. Cai, M. Liu, M. Zhao, B. Chen, Q. Chen, and Z. Hu, (2021) *"Pile-Soil Stress Ratio and Settlement of Composite Foundation Bidirectionally Reinforced by Piles and Geosynthetics under Embankment Load"* **Advances in Civil Engineering *2021***(1): 5575878. DOI: 10.1155/2021/5575878.

[13] S. Nurdin, K. Sawada, and S. Moriguchi. "Design criterion of reinforcement on thick soft clay foundations of traditional construction method in Indonesia". In: ***258***. EDP Sciences, 2019, 03010. DOI: 10.1051/matecconf/201925803010.

[14] E. Momeni, R. Nazir, D. J. Armaghani, and H. Maizir, (2014) *"Prediction of pile bearing capacity using a hybrid genetic algorithm-based ANN"* **Measurement *57***: 122–131. DOI: 10.1016/j.measurement.2014.08.007.

[15] T. A. Pham, H.-B. Ly, V. Q. Tran, L. V. Giap, H.-L. T. Vu, and H.-A. T. Duong, (2020) *"Prediction of pile axial bearing capacity using artificial neural network and random forest"* **Applied Sciences *10***: 1871. DOI: 10.3390/app10051871.

[16] T. A. Pham, V. Q. Tran, H.-L. T. Vu, and H.-B. Ly, (2020) *"Design deep neural network architecture using a genetic algorithm for estimation of pile bearing capacity"* **PLoS One *15***: e0243030. DOI: 10.1371/journal.pone.0243030.

[17] N. Shariatmadari, A. A. ESLAMI, and P. F. M. KARIM, (2008) *"Bearing capacity of driven piles in sands from SPT–applied to 60 case histories"* ***32***: 125–140. DOI: 10.22099/ijstc.2008.716.

[18] M. R. Svinkin, (2019) *"Sensible determination of pile capacity by dynamic methods"* **Geotechnical research *6***: 52–67. DOI: 10.1680/jgere.18.00032.

[19] H. Nguyen, M.-T. Cao, X.-L. Tran, T.-H. Tran, and N.-D. Hoang, (2023) *"A novel whale optimization algorithm optimized XGBoost regression for estimating bearing capacity of concrete piles"* **Neural Computing and Applications *35***: 3825–3852. DOI: 10.1007/s00521-022-07896-w.

[20] F. P. Nejad, M. B. Jaksa, M. Kakhi, and B. A. McCabe, (2009) *"Prediction of pile settlement using artificial neural networks based on standard penetration test data"* **Computers and geotechnics *36***: 1125–1133. DOI: 10.1016/j.compgeo.2009.04.003.

[21] A. T. C. Goh, F. H. Kulhawy, and C. G. Chua, (2005) *"Bayesian neural network analysis of undrained side resistance of drilled shafts"* **Journal of Geotechnical and Geoenvironmental Engineering *131***: 84–93. DOI: 10.1061/(ASCE)1090-0241(2005)131:1(84).

[22] M. A. Shahin and M. B. Jaksa, (2005) *"Neural network prediction of pullout capacity of marquee ground anchors"* **Computers and Geotechnics *32***: 153–163. DOI: 10.1016/j.compgeo.2005.02.003.

[23] N. O. Nawari, R. Liang, and J. Nusairat, (1999) *"Artificial intelligence techniques for the design and analysis of deep foundations"* **Electronic Journal of Geotechnical Engineering *4***: 1–21.

[24] V.-H. Nhu, N.-D. Hoang, V.-B. Duong, H.-D. Vu, and D. T. Bui, (2020) *"A hybrid computational intelligence approach for predicting soil shear strength for urban housing construction: a case study at Vinhomes Imperia project, Hai Phong city (Vietnam)"* **Engineering with Computers *36***: 603–616. DOI: 10.1007/s00366-019-00718-z.

[25] B. T. Pham, C. Qi, L. S. Ho, T. Nguyen-Thoi, N. Al-Ansari, M. D. Nguyen, H. D. Nguyen, H.-B. Ly, H. V. Le, and I. Prakash, (2020) *"A novel hybrid soft computing model using random forest and particle swarm optimization for estimation of undrained shear strength of soil"* **Sustainability *12***: 2218. DOI: 10.3390/su12062218.

[26] E. Momeni, D. J. Armaghani, S. A. Fatemi, and R. Nazir, (2018) *"Prediction of bearing capacity of thin-walled foundation: a simulation approach"* **Engineering with Computers *34***: 319–327. DOI: 10.1007/s00366-017-0542-x.

[27] E. Momeni, M. B. Dowlatshahi, F. Omidinasab, H. Maizir, and D. J. Armaghani, (2020) *"Gaussian process regression technique to estimate the pile bearing capacity"* **Arabian Journal for Science and Engineering *45***: 8255–8267. DOI: 10.1007/s13369-020-04683-4.

[28] R. U. Kulkarni and D. M. Dewaikar, (2017) *"Prediction of interpreted failure loads of rock-socketed piles in Mumbai Region using hybrid artificial neural networks with genetic algorithm"* **Int. J. Eng. Res *6***: 365–372. DOI: 10.17577/IJERTV6IS060196.

[29] D. J. Armaghani, R. S. N. S. B. R. Shoib, K. Faizi, and A. S. A. Rashid, (2017) *"Developing a hybrid PSO–ANN model for estimating the ultimate bearing capacity of rock-socketed piles"* **Neural Computing and Applications *28***: 391–405. DOI: 10.1007/s00521-015-2072-z.

[30] L. Wang, Q. Cao, Z. Zhang, S. Mirjalili, and W. Zhao, (2022) *"Artificial rabbits optimization: A new bio-inspired meta-heuristic algorithm for solving engineering optimization problems"* **Engineering Applications of Artificial Intelligence *114***: 105082. DOI: 10.1016/j.engappai.2022.105082.

[31] V. Hayyolalam and A. A. P. Kazem, (2020) *"Black widow optimization algorithm: a novel meta-heuristic approach for solving engineering optimization problems"* **Engineering Applications of Artificial Intelligence *87***: 103249. DOI: 10.1016/j.engappai.2019.103249.

[32] E. H. Houssein, M. M. Emam, and A. A. Ali, (2021) *"An efficient multilevel thresholding segmentation method for thermography breast cancer imaging based on improved chimp optimization algorithm"* **Expert Systems with Applications *185***: 115651. DOI: 10.1016/j.eswa.2021.115651.

[33] N. A. Munirah, M. A. Remli, N. M. Ali, H. W. Nies, M. S. Mohamad, and K. N. S. W. S. Wong, (2020) *"The development of parameter estimation method for Chinese hamster ovary model using black widow optimization algorithm"* **International Journal of Advanced Computer Science and Applications *11***: DOI: 10.14569/IJACSA.2020.0111126.

[34] C. Cortes and V. Vapnik, (1995) *"Support-vector networks"* **Machine learning *20***: 273–297. DOI: 10.1007/BF00994018.

[35] M.-T. Puth, M. Neuhäuser, and G. D. Ruxton, (2014) *"Effective use of Pearson's product–moment correlation coefficient"* **Animal behaviour *93***: 183–189. DOI: 10.1016/j.anbehav.2014.05.003.